**Contemporary Cardiology**
*Series Editor:* Peter P. Toth

Gan-Xin Yan
Peter R. Kowey
Charles Antzelevitch *Editors*

# Management of Cardiac Arrhythmias

*Third Edition*

Humana Press

# Contemporary Cardiology

**Series Editor**

Peter P. Toth
Ciccarone Center for the Prevention of Cardiovascular Disease
Johns Hopkins University School of Medicine
Baltimore, MD
USA

For more than a decade, cardiologists have relied on the Contemporary Cardiology series to provide them with forefront medical references on all aspects of cardiology. Each title is carefully crafted by world-renown cardiologists who comprehensively cover the most important topics in this rapidly advancing field. With more than 75 titles in print covering everything from diabetes and cardiovascular disease to the management of acute coronary syndromes, the Contemporary Cardiology series has become the leading reference source for the practice of cardiac care.

More information about this series at http://www.springer.com/series/7677

Gan-Xin Yan • Peter R. Kowey
Charles Antzelevitch
Editors

# Management of Cardiac Arrhythmias

Third Edition

Humana Press

*Editors*
Gan-Xin Yan
Lankenau Heart Institute
Thomas Jefferson University
Wynnewood, PA
USA

Peter R. Kowey
Lankenau Heart Institute
Thomas Jefferson University
Wynnewood, PA
USA

Charles Antzelevitch
Lankenau Heart Institute
Thomas Jefferson University
Wynnewood, PA
USA

ISSN 2196-8969 ISSN 2196-8977 (electronic)
Contemporary Cardiology
ISBN 978-3-030-41966-0 ISBN 978-3-030-41967-7 (eBook)
https://doi.org/10.1007/978-3-030-41967-7



This Humana imprint is published by the registered company Springer Nature Switzerland AG
The registered company address is: Gewerbestrasse 11, 6330 Cham, Switzerland

# Contents

# Contributors

**Michael J. Ackerman, MD, PhD** Department of Pediatrics (Division of Pediatric Cardiology), Departments of Cardiovascular Medicine (Division of Heart Rhythm Services), Pediatrics (Division of Pediatric Cardiology), and Molecular Pharmacology & Experimental Therapeutics (Windland Smith Rice Sudden Death Genomics Laboratory, Genetic Heart Rhythm Clinic), Mayo Clinic, Rochester, MN, USA

**Wayne O. Adkisson, MD** Cardiac Arrhythmia and Syncope Center, Cardiovascular Division, Department of Medicine, University of Minnesota Medical School, Minneapolis, MN, USA

**Amin Al-Ahmad, MD** Texas Cardiac Arrhythmia Institute, St. David's Medical Center, Austin, TX, USA

Arrhythmia and Electrophysiology Unit, Department of Cardiology, Hacettepe University Hospitals, Ankara, USA

**Mohamed Al-Rawahi, MD, FRCPC, FACC, FHRS** Cardiac Electrophysiology Section, Cardiovascular Division, Hospital of the University of Pennsylvania and University of Pennsylvania School of Medicine, Philadelphia, PA, USA

Cardiology unit, Department of Medicine, Sultan Qaboos University Hospital, Seeb, Oman

**Charles Antzelevitch, PhD, FACC, FHRS, FAHA** Lankenau Institute for Medical Research, Wynnewood, PA, USA

Lankenau Heart Institute, Wynnewood, PA, USA

Sidney Kimmel Medical College of Thomas Jefferson University, Philadelphia, PA, USA

**Hector Barajas-Martinez, PhD** Cardiovascular Research, Lankenau Institute for Medical Research, Wynnewood, PA, USA

**David G. Benditt, BScEE, MD** Cardiac Arrhythmia and Syncope Center, Cardiovascular Division, Department of Medicine, University of Minnesota Medical Schoo, Minneapolis, MN, USA

**Aditya Bhonsale, MD** Heart and Vascular Institute, University of Pittsburgh Medical Center, University of Pittsburgh School of Medicine, Pittsburgh, PA, USA

**Sylvia Marie R. Biso, MD** Department of Medicine, Division of Cardiology, University of Illinois at Chicago and Jesse Brown Veterans Administration, Chicago, IL, USA

**Alexander Burashnikov, PhD** Lankenau Institute for Medical Research, Wynnewood, PA, USA

Sidney Kimmel Medical College of Thomas Jefferson University, Philadelphia, PA, USA

**J. David Burkhardt, MD** Texas Cardiac Arrhythmia Institute, St. David's Medical Center, Austin, TX, USA

**David J. Callans, MD** Division of Cardiovascular Medicine, Department of Medicine, Hospital of the University of Pennsylvania, University of Pennsylvania Health System, Philadelphia, PA, USA

**Ilknur Can, MD** Cardiac Arrhythmia and Syncope Center, Cardiovascular Division, Department of Medicine, University of Minnesota Medical School, Minneapolis, MN, USA

**Uğur Canpolat, MD** Texas Cardiac Arrhythmia Institute, St. David's Medical Center, Austin, TX, USA

Arrhythmia and Electrophysiology Unit, Department of Cardiology, Hacettepe University Hospitals, Ankara, Turkey

**Qiong Chen** Texas Cardiac Arrhythmia Institute, St. David's Medical Center, Austin, TX, USA

Department of Cardiopulmonary Function Test, Henan Provincial People's Hospital, People's Hospital of Zhengzhou University, Zhengzhou, China

**Ka Hou Christien Li, MBBS, FESC** Faculty of Medicine, Newcastle University, Newcastle, UK

**Alberto Cipriani, MD** Department of Cardiac, Thoracic and Vascular Sciences, University of Padua Medical School, Padua, Italy

**Domenico Corrado, MD, PhD, FESC** Department of Cardiac, Thoracic and Vascular Sciences, University of Padua Medical School, Padua, Italy

**Dawood Darbar, MB, ChB, MD** Department of Medicine, Division of Cardiology, University of Illinois at Chicago and Jesse Brown Veterans Administration, Chicago, IL, USA

**Domenico G. Della Rocca, MD** Texas Cardiac Arrhythmia Institute, St. David's Medical Center, Austin, TX, USA

**Isabelle Denjoy, MD** AP-HP, Hôpital Bichat, Département de Cardiologie et Centre de Référence des Maladies Cardiaques Héréditaires, Paris, France

Université de Paris INSERM U1166, Paris, France

**Rahul Dhawan, MD** Division of Cardiovascular Medicine, Department of Internal Medicine, University of Nebraska Medical Center, Omaha, NE, USA

**José M. Di Diego, MD** Cardiovascular Research Group, Lankenau Institute for Medical Research, Wynnewood, PA, USA

**Igor R Efimov, PhD** Department of Biomedical Engineering, The George Washington University, Washington, DC, USA

**Alan D. Enriquez, MD** Department of Cardiovascular Medicine, Yale University School of Medicine, New Haven, CT, USA

**Douglas Esberg, MD** Lankenau Medical Center, Wynnewood, PA, USA

**N. A. Mark Estes III, MD** Heart and Vascular Institute, University of Pittsburgh School of Medicine, Pittsburgh, PA, USA

**John Field, MD** Department of Medicine, Penn State University College of Medicine – Hershey, Hershey Medical Center Penn State University, Hershey, PA, USA

**Thomas Fink, MD** University Heart Center Lübeck, Department of Cardiology, Angiology, and Intensive Care Medicine, University Hospital Schleswig-Holstein, Lübeck, Germany

**Sharon Ann George, PhD** Department of Biomedical Engineering, The George Washington University, Washington, DC, USA

**Carola Gianni, MD** Texas Cardiac Arrhythmia Institute, St. David's Medical Center, Austin, TX, USA

**John R. Giudicessi, MD, PhD** Department of Cardiovascular Medicine (Clinician-Investigator Training Program), Mayo Clinic, Rochester, MN, USA

**Matthew A. Goldstein, BA, MD** Department of Cardiology, Paoli Hospital, Paoli, PA, USA

**Rakesh Gopinathannair, MD, MA, FAHA, FHRS** Kansas City Heart Rhythm Institute, Overland Park, KS, USA

University of Missouri-Columbia, Columbia, MO, USA

**Gustavo S. Guandalini, MD** Division of Cardiovascular Medicine, Department of Medicine, Hospital of the University of Pennsylvania, University of Pennsylvania Health System, Philadelphia, PA, USA

**E. Kevin Heist, MD, PhD** Cardiac Electrophysiology Fellowship Program, Heart Center, Corrigan Minehan Heart Center, Massachusetts General Hospital, Boston, MA, USA

**Kathleen Hickey, RN, DNP** Department of Medicine, Division of Cardiology, Columbia University Medical Center, New York, NY, USA

**Kui Hong, MD, PhD** Department of Cardiovascular Medicine, The Second Affiliated Hospital of Nanchang University, Nanchang, China

**Hideki Itoh, MD, PhD** Department of Cardiovascular Medicine, Shiga University of Medical Science, Otsu, Shiga, Japan

Division of Patient Safety, Hiroshima University Hospital, Hiroshima, Japan

**Yong Jiang, MD** Department of Electrocardiogram, The First Affiliated Hospital of Jishou University, Jishou, China

**Youssef Jalloul, MD** Cardiology Division/Cardiac Electrophysiology Section, Department of Internal Medicine, American University of Beirut Faculty of Medicine and Medical Center, Beirut, Lebanon

**Ronald J. Kanter, MD** Department of Cardiology, Nicklaus Children's Hospital, Miami, FL, USA

**Amanulla Khaji, MD, FACC** Lankenau Medical Center, Wynnewood, PA, USA

**Eun-jeong Kim, MD** Vanderbilt Heart and Vascular Institute, Vanderbilt University Medical Center, Nashville, TN, USA

**Bradley P. Knight, MD** Department of Electrophysiology, Northwestern Medicine, Northwestern University, Chicago, IL, USA

Bluhm Cardiovascular Institute at Northwestern Memorial Hospital, Chicago, IL, USA

**Panagiotis Korantzopoulos, MD, PhD** First Department of Cardiology, University of Ioannina Faculty of Medicine, Ioannina, Greece

**Antoine Leenhardt, MD** AP-HP, Hôpital Bichat, Département de Cardiologie et Centre de Référence des Maladies Cardiaques Héréditaires, Paris, France

Université de Paris INSERM U1166, Paris, France

**Wei Li, MD, PhD** Department of Cardiology, Xinhua Hospital, School of Medicine, Shanghai Jiao Tong University, Shanghai, China

**Yi-Gang Li, MD** Department of Cardiology, Xinhua Hospital, School of Medicine, Shanghai Jiao Tong University, Shanghai, China

**Krystien V. V. Lieve, MD** AMC Heart Center, Department of Clinical and Experimental Cardiology, Academic Medical Center, Amsterdam, the Netherlands

**Zexu Lin, MS** Department of Biomedical Engineering, The George Washington University, Washington, DC, USA

**Mark S. Link, MD** Division of Cardiology, UT Southwestern Medical Center, Dallas, TX, USA

Cardiac Arrhythmia Services, University of Texas Southwestern, Dallas, TX, USA

**Tong Liu, MD, PhD** Tianjin Key Laboratory of Ionic-Molecular Function of Cardiovascular Disease, Department of Cardiology, Tianjin Institute of Cardiology, The Second Hospital of Tianjin Medical University, Tianjin, China

**Xing-Bin Liu, MD, FHRS** Department of Cardiology, West China Hospital, Sichuan University, Chengdu, People's Republic of China

**Michael M. Lopez, MD** Department of Cardiology, Nicklaus Children's Hospital, Miami, FL, USA

**Abhishek Maan, MD, ScM** Department of Cardiac Electrophysiology, Corrigan Minehan Heart Center, Massachusetts General Hospital, Boston, MA, USA

**Alice Maltret, MD** Unité médico-chirurgicale de cardiologie congénitale et pédiatrique, M3C-Necker, Hôpital Universitaire Necker Enfants Malades, Université Paris Descartes, Sorbonne Paris Cité, Paris, France

**Moussa Mansour, MD** Cardiac Arrhythmia Service, Heart Center, Corrigan Minehan Heart Center, Harvard Medical School, Massachusetts General Hospital, Boston, MA, USA

**Francis E. Marchlinski, MD** Cardiac Electrophysiology Section, Cardiovascular Division, Hospital of the University of Pennsylvania and University of Pennsylvania School of Medicine, Philadelphia, PA, USA

Department of Cardiac Electrophysiology, University of Pennsylvania Health System, Philadelphia, PA, USA

**Giulia Mattesi, MD** Department of Cardiac, Thoracic and Vascular Sciences, University of Padua Medical School, Padua, Italy

**Shayna McEnteggart, BS** University of Central Florida College of Medicine, Orlando, FL, USA

**Gregory F. Michaud, MD** Division of Arrhythmia, Vanderbilt Heart and Vascular Institute, Vanderbilt University Medical Center, Nashville, TN, USA

**Gerald V. Naccarelli, MD** Division of Cardiology, Penn State Hershey Heart & Vascular Institute, Penn State University College of Medicine – Hershey, Hershey, PA, USA

**Niyada Naksuk, MD** Department of Medicine, Division of Cardiology, University of Illinois at Chicago and Jesse Brown Veterans Administration, Chicago, IL, USA

**Andrea Natale, MD** Texas Cardiac Arrhythmia Institute, St. David's Medical Center, Austin, TX, USA

HCA National Medical Director of Cardiac Electrophysiology, USA

Interventional Electrophysiology, Scripps Clinic, La Jolla, CA, USA

MetroHealth Medical Center, Case Western Reserve University School of Medicine, Cleveland, OH, USA

**Feifan Ouyang, MD** Cardiac Arrhythmia Center, National Center of Cardiovascular Diseases/Fuwai Hospital, Peking Union Medical College/the Chinese Academy of Medical Sciences, Beijing, China

**Marwan M. Refaat, MD** Cardiology Division/Cardiac Electrophysiology Section, Department of Internal Medicine, American University of Beirut Faculty of Medicine and Medical Center, Beirut, Lebanon

**Michael Rehorn, MD** Clinical Cardiac Electrophysiology, Cardiology Division, Department of Medicine, Duke University Medical Center, Durham, NC, USA

**James A. Reiffel, MD** Department of Medicine, Division of Cardiology, Columbia University Medical Center, New York, NY, USA

**Steven A. Rothman, MD** Department of Cardiovascular Medicine, Lankenau Medical Center, Wynnewood, PA, USA

**Deepak Saluja, MD** Department of Medicine, Division of Cardiology, Columbia University Medical Center, New York, NY, USA

**Wataru Shimizu, MD, PhD** Department of Cardiovascular Medicine, Graduate School of Medicine, Nippon Medical School, Tokyo, Japan

**Albert Y. Sun, MD** Clinical Cardiac Electrophysiology, Cardiology Division, Department of Medicine, Duke University Medical Center, Durham, NC, USA

**Usha B. Tedrow, MD, MSc** Cardiovascular Division, Brigham and Women's Hospital, Boston, MA, USA

**Amar Trivedi, MD** Department of Cardiac Electrophysiology, Northwestern Memorial Hospital, Chicago, IL, USA

**Gary Tse, MD, PhD, FRCP** Tianjin Key Laboratory of Ionic-Molecular Function of Cardiovascular Disease, Department of Cardiology, Tianjin Institute of Cardiology, The Second Hospital of Tianjin Medical University, Tianjin, China

**Christian van der Werf, MD, PhD** AMC Heart Center, Department of Clinical and Experimental Cardiology, Academic Medical Center, Amsterdam, the Netherlands

**Jianyong Wang, MM** Department of Electrophysiology, TEDA International Cardiovascular Hospital, Tianjin, China

**Gan-Xin Yan, MD, PhD, FACC** Department of Cardiology, Lankenau Institute for Medical Research and Lankenau Medical Center, Wynnewood, PA, USA

Sidney Kimmel College of Medicine, Thomas Jefferson University, Philadelphia, PA, USA

Department of Cardiology, Fuwai Huazhong Hospital, Zhengzhou, China

**Jian-hua Yu, MD, PhD** Department of Cardiovascular Medicine, The Second Affiliated Hospital of Nanchang University, Nanchang, China

**Ping Yu** Department of Cardiology, Jiangsu Province Hospital, Nanjing, China

**Shu Zhang, MD, PhD** Cardiac Arrhythmia Center, National Center of Cardiovascular Diseases/Fuwai Hospital, Peking Union Medical College/the Chinese Academy of Medical Sciences, Beijing, China

**Yubin Zhang, BS** Department of Cardiology, Department of Electrocardiogram, The First Affiliated Hospital, School of Medicine, Zhejiang University, Hangzhou, China

**Alessandro Zorzi, MD, PhD, FESC** Department of Cardiac, Thoracic and Vascular Sciences, University of Padua Medical School, Padua, Italy

# Part I

# Basic Principles of Cardiac Electrophysiology and Pharmacology

# Basic Principles of Cardiac Electrophysiology

1

Sharon Ann George, Zexu Lin, and Igor R Efimov

## Introduction

Cardiac tissue is an electrical syncytium, the coordinated stimulation of which allows for the contraction of the tissue, for the effective pumping action of the heart. Each individual cardiomyocyte is an electrically excitable cell and its electrical properties and proteins that contribute to its function differ depending on the type of cardiomyocyte and its location in the heart. This chapter discusses the major ion channels that contribute to the electrical activity of cardiomyocytes, action potential and its heterogeneity, intercellular electrical coupling, and conduction of the action potentials.

## Resting Membrane Potential

Membrane potential ($V_m$), also known as transmembrane potential (measured in millivolts, mV), is the difference in electric potential between the inside and outside of a cell. At resting conditions (i.e., without stimulation), the inside of a cardiomyocyte has a negative potential compared to the outside, resulting in a *resting membrane potential* (RMP) of approximately −85 to −90 mV in ventricular cardiomyocytes. RMP is achieved by a fine balance of several ions between the inside and outside of the cell membrane.

Under normal physiological conditions, intracellular (inside the cell) potassium ion ($K^+$) concentration is higher than the extracellular concentration, whereas the opposite is true for sodium ion ($Na^+$) concentrations, i.e., the intracellular $Na^+$ ion concentration is lesser than the extracellular concentration. Also important are

S. A. George (✉) · Z. Lin · I. R. Efimov
Department of Biomedical Engineering, The George Washington University, Washington, DC, USA
e-mail: sharonag@gwu.edu


G.-X. Yan et al. (eds.), *Management of Cardiac Arrhythmias*, Contemporary Cardiology, https://doi.org/10.1007/978-3-030-41967-7_1

**Table 1.1** Intracellular and extracellular ion concentrations in mammalian cardiomyocytes [1]

| Ions | Intracellular concentration (mM) | Extracellular concentration (mM) |
|---|---|---|
| $Na^+$ | 15 | 142 |
| $K^+$ | 150 | 4 |
| $Cl^-$ | 5 | 120 |
| $Ca^{2+}$ | $10^{-4}$ | 1 |
| $Mg^+$ | 1 | 0.5 |
| $HCO_3^{-1}$ | 8 | 27 |
| Non-penetrating anions | 155 | 0 |

various negatively charged intracellular proteins that cannot cross the cell membrane. A summary of approximate ion concentrations inside and outside mammalian cardiomyocytes is given in Table 1.1.

The difference in ion concentrations across the cell membrane sets up an electrical and chemical gradient or an *electrochemical gradient*. The electrical gradient is a result of the charge carried by ions, whereas the chemical gradient is a result of their concentration differences across the cell membrane. The movement of ions across the cell membrane results in an *ionic current*. Taking only one ion species into consideration, if the cell membrane is permeable to that ion, it'll continue to flow across the cell membrane until its electrical gradient balances out the chemical gradient. The potential at which this occurs is called the equilibrium potential or *Nernst potential* of that ion and the net flux of that particular ion across the cell membrane becomes zero. In order to determine the Nernst potential, let's first consider the Gibbs free energy equation:

$$\Delta G = \underbrace{RTln\left(\frac{[X]_o}{[X]_i}\right)}_{\substack{\text{energy in} \\ \text{chemical gradient}}} - \underbrace{Z_X F E_X}_{\substack{\text{energy} \\ \text{in} \\ \text{electrical gradient}}}$$

When chemical gradient balances out electrical gradient, $\Delta G = 0$, and the Nernst potential is calculated by solving the following equation:

$$0 = RTln\left(\frac{[X]_o}{[X]_i}\right) - Z_X F E_X$$

Finally, the Nernst potential for one ion species can by calculated as:

$$E_X = \frac{RT}{Z_X F} \ln\left(\frac{[X]_o}{[X]_i}\right) \quad \text{Nernst equation}$$

where

$E_X$ is the equilibrium potential for ion species $X$

$R$ is the gas constant (8.314 $J.K^{-1}.mol^{-1}$ joules per kelvin per mole)

$T$ is the absolute temperature on the Kelvin scale ($K$ = °C + 273.15)

$Z_X$ is the valency of ion species X (e.g., $Z_{Ca} = +2$ for $Ca^{2+}$, $Z_{Cl} = -1$ for $Cl^-$)
$F$ is the Faraday's constant (96,485 C.mol$^{-1}$ coulombs per mole)
$[X]_O$ is the extracellular concentration of ion species $X$
$[X]_i$ is the intracellular concentration of ion species $X$

The equilibrium potential for several biologically relevant ions can be calculated as:

$$E_K = \frac{RT}{F}\ln\left(\frac{[K]_O}{[K]_i}\right) \quad E_{Na} = \frac{RT}{F}\ln\left(\frac{[Na]_O}{[Na]_i}\right) \quad E_{Ca} = \frac{RT}{2F}\ln\left(\frac{[Ca]_O}{[Ca]_i}\right)$$

Substituting the known constants and the extracellular and intracellular ion concentrations from Table 1.1 in the equation above, we can calculate the Nernst potential for potassium ions, $E_K$, as −96 mV. This means that, at a membrane potential of −96 mV, there will be zero net $K^+$ flux, as $K^+$ is in electrochemical balance across the membrane. Similarly, $E_x$ for other ions can also be determined as $E_{Na}$ = +60 mV and $E_{Ca}$ = +123.01 mV.

When the cell membrane is more permeable to one ion species compared to others, the flow of that ion across the cell membrane will bring the membrane potential closer to the Nernst potential of that ion. For example, at RMP, the cell membrane is more permeable to potassium ions; therefore, RMP is closer to $E_K$ for most cardiac cells. However, other ion currents can also contribute to RMP, and a more accurate estimate of membrane potential is obtained from the *Goldman-Hodgkin-Katz equation* (GHK equation) which takes into account the relative contributions of several ion species. For a cardiomyocyte, when the membrane is permeable to $K^+$, $Na^+$, and $Cl^-$, the GHK equation can be expressed as:

$$E_m = \frac{RT}{F}\ln\left(\frac{p_K[K]_O + p_{Na}[Na]_O + p_{Cl}[Cl]_i}{p_K[K]_i + p_{Na}[Na]_i + p_{Cl}[Cl]_o}\right) \quad \text{GHK equation}$$

where
$E_m$ is the membrane potential
$R$ is the gas constant (8.314 J.K$^{-1}$.mol$^{-1}$ joules per kelvin per mole)
$T$ is the absolute temperature on the Kelvin scale ($K$ = °C + 273.15)
$F$ is the Faraday's constant (96,485 C.mol$^{-1}$ coulombs per mole)
$p_X$ is the membrane permeability for ion species $X$
$[X]_O$ is the extracellular concentration of ion species $X$
$[X]_i$ is the intracellular concentration of ion species $X$

Note, to account for the differences in valency, the $Cl^-$ concentrations are presented as "out over in" in the equation since $Cl^-$ has a valency of −1.

If the cell membrane is only permeable to one specific ion species, then the GHK equation simplifies to Nernst equation of that particular ion. In summary, the combination of ion gradients across the membrane and the selective membrane permeability to different ion species determine the RMP.

## Ion Channels

Ions cannot freely diffuse across cell membrane; they can only cross the cell membrane through specialized membrane-spanning proteins such as ion channels and transporters (or carriers). Ion channels are pore-forming membrane proteins that allow ions to passively flow through the channel pore, down the electrochemical gradient. Generally, ion channels have a tetrameric structure in which four protein subunits construct a central ion conducting pore structure (i.e., α-subunit) with auxiliary subunits (i.e., β-subunits) around it modulating channel functions [2]. Many ion channels are highly selective to one type of ion and as such are named after the ions that they conduct, for example, $Na^+$, $K^+$, or $Ca^{2+}$ion channels. This ion selectivity is due to an ion selective filter in the pore structure that only allows one specific ion species through it. The function of several ion channels depend on voltage across the cell membrane (voltage-gated ion channels) or binding of ligands (ligand-gated ion channels), which control gating mechanisms that either open or close an ion channel. Ion channels are critical for physiological rhythmicity and contractility of the heart. They are also the pharmacological targets in cardiac diseases such as ventricular fibrillation or angina. The overall structure and properties of $Na^+$, $Ca^{2+}$, and $K^+$ channels are discussed here.

## Sodium Ion Channels

### Structure

Voltage-gated $Na^+$ channels ($Na_V$) have a large pore-forming *α-subunit* (~260 kDa) that determines the principal electrophysiological and pharmacological properties of the $Na^+$ channels (Fig. 1.1). Different α-subunits define the

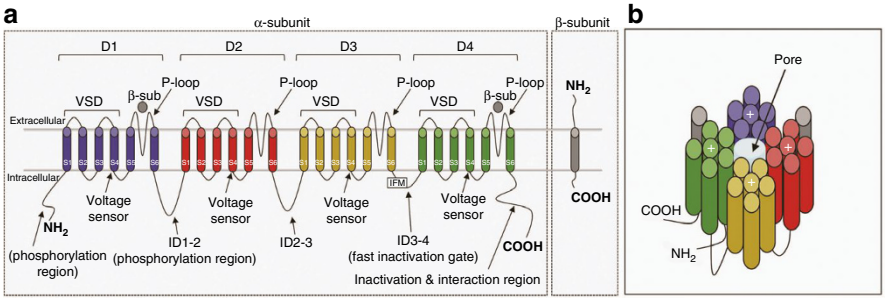


**Fig. 1.1** (**a**) Schematic representation of the $Na_V1.5$ cardiac sodium channel [4]. IFM is the fast inactivation region represented by isoleucine, phenylalanine, and methionine; the gray circle represents the β-subunit interaction region; VSD is the voltage sensing domain; ID1–2, ID2–3, and ID3–4 are the interdomain linkers. On the right is a schematic representation of the β-subunit. (**b**) Schematic three-dimensional representation of $Na_V1.5$. The blue, red, yellow, and green blocks represent domains I, II, III, and IV, respectively. The gray blocks represent β-subunits. The light blue circle represents the aqueous pore. (Reprinted from Detta et al. [4], with permission from Elsevier)

different isoforms of $Na_v$ channels. $Na_v$ channels also have one to two auxiliary or regulatory units called β-*subunits* that modulate the function of the α-subunit [3, 4]. To date, four types of β-subunits (β1–β4) have been identified and are classified into two groups: the first group includes β1 (expressed in the brain, skeletal muscle, and heart) and β3 (expressed in neuronal tissue); and the second group includes β2 and β4 [5].

The α-subunits of $Na_V$ channels are composed of four homologous transmembrane domains (DI–IV) connected by intracellular linking peptide segments. Each domain contains six α-helical transmembrane peptide segments (S1–S6) and a pore (P) loop between S5 and S6. The P loops from the four domains together line the extracellular pore of $Na_V$ channels and are important for the ion selectivity of channels and also act as the binding site of natural toxins such as puffer fish poison tetrodotoxin [3, 6]. The Asp-Glu-Lys-Ala motif in the α-subunit of $Na_V$ channels determines $Na^+$ *selectivity* [7].

Segments S1–S4 form the *voltage sensing domain* (VSD) regulate channel function. The S4 segment contains positively charged amino acid residues which act as the *voltage sensor* of the $Na_V$ channel. At RMP, the channel is closed because of the inward position (toward the pore) of the S4 segments. The depolarization of membrane (i.e., the shift of membrane potential from negative to positive potential) results in a transient outward movement of S4 segments which opens the channel [8]. The intracellular peptide chain that connects the S6 segment of domain III to the S1 segment of domain IV forms the *inactivation gate*. Following the depolarization-induced opening of the $Na_V$ channels, the inactivation gate occludes the central pore structure from the cytoplasmic side during sustained depolarization [9, 10] to inactivate the channel.

## Nomenclature and Family of $Na_v$ Channels

Nine different types of $Na_V$ channels have been identified via electrophysiological recording and biochemical purification and cloning; they are named with different numbers based on amino acid sequence similarities of the α-subunits (Table 1.2) [11]. Take "$Na_V1.5$" as an example:

| $Na_V1.5$ | | | |
|---|---|---|---|
| Na | V | 1 | 5 |
| The principal permeating ion | The principal physiological regulator | The gene subfamily (currently only $Na_v1$) | The specific channel isoform |

Note the last number (e.g., "5") is assigned based on the order in which the channels were identified, while the splice variants of each subtype are identified by lowercase letters at the end (e.g., $Na_V1.1a$).

For more detailed information on $Na_V$ channels such as gene and protein information, voltage dependence, channel activator and inhibitor, channel blockers, species and tissue distribution, and clinically relevant mutations and pathophysiology, please refer to the International Union of Basic and Clinical Pharmacology (IUPHAR) voltage-gated sodium channels database [12].

**Table 1.2** Summary of human voltage-gated sodium channels [13, 14]

| Channel | Gene | Chromosome location | Tissue distribution | Tetrodotoxin sensitivity |
|---|---|---|---|---|
| $Na_V1.1$ | SCN1A | 2q24.3 | Spinal neurons, primarily cell bodies, brain neurons | Sensitive |
| $Na_V1.2$ | SCN2A | 2q22–23 | Brain, neuronal cell bodies and dendrites | Sensitive |
| $Na_V1.3$ | SCN3A | 2q23–24 | Spinal cord, thalamus, amygdala, cerebellum, adult and fetal whole brain and heart | Sensitive |
| $Na_V1.4$ | SCN4A | 17q23–25 | Skeletal muscle | Sensitive |
| $Na_V1.5$ | SCN5A | 3p21 | Heart, immature and denervated skeletal muscles, certain brain neurons | Resistant |
| $Na_V1.6$ | SCN8A | 12q13 | Brain neurons | Sensitive |
| $Na_V1.7$ | SCN9A | 2q24 | Dorsal root ganglia neurons, sympathetic neurons, Schwann cells, neuroendocrine cells | Sensitive |
| $Na_V1.8$ | SCN10A | 3p22–p21 | Dorsal root ganglia neurons, heart, intracardiac neurons | Resistant |
| $Na_V1.9$ | SCN11A | 3p22.2 | C-type neurons in dorsal root ganglia | Resistant |

## Voltage-Gated Sodium Ion Channels

$Na_V$ channels are responsible for the fast inward $Na^+$ current ($I_{Na}$) which generates the fast depolarization of cardiomyocytes and other excitable cells, including neurons and skeletal muscle cells. $Na_V$ channels are also important targets for class I anti-arrhythmic agents based on Vaughan-Williams scheme[15]. $Na_V$ channels have three functional states: closed (or *deactivated*) state at RMP, open (or *activated*) state during the first few milliseconds of depolarization, and nonconducting (or *inactivated*) state after the initial depolarization and during repolarization [16]. Once activated there is a rapid inward $Na^+$ current through the channel pore because of the higher extracellular $Na^+$ concentration (relative to intracellular $Na^+$ concentration). Immediately after activation, the channels become inactivated and the pore is closed again. During inactivated state, $Na_v$ channels cannot respond to stimuli (i.e., conduct $Na^+$) and this state determines the absolute refractory period. The recovery from inactivation takes place gradually during membrane repolarization which is called the voltage- and time-dependent recovery of $Na_V$ channels [17].

$Na_V1.5$: $Na_V1.5$ is the predominant $Na_V$ channel isoform in the heart, expressed in the atrial and ventricular myocytes, in the Purkinje fibers, and to a lesser extent in the sinoatrial (SA) and atrioventricular (AV) nodes [18]. $Na_V1.5$ is encoded by the SCN5A gene located on chromosome 3p21 and consists of 28 exons [19]. $Na_v1.5$ activation plays a critical role in initiating the cardiac action potential (AP) and the resultant activation of voltage-gated calcium channels ($Ca_v$). Mutations in the human SCN5A gene have been related to multiple disturbances in cardiac function and include loss-of-function mutations (Brugada syndrome type I) and gain-of-function mutations (long QT syndrome type 3) [20, 21].

Figure 1.2 illustrates the properties of the current associated with the $Na_v1.5$ channel, $I_{Na}$, and the changes associated with a mutation (1493delK) in the channel. The $I_{Na}$ traces, corresponding averaged current-voltage (I-V) relationships, and

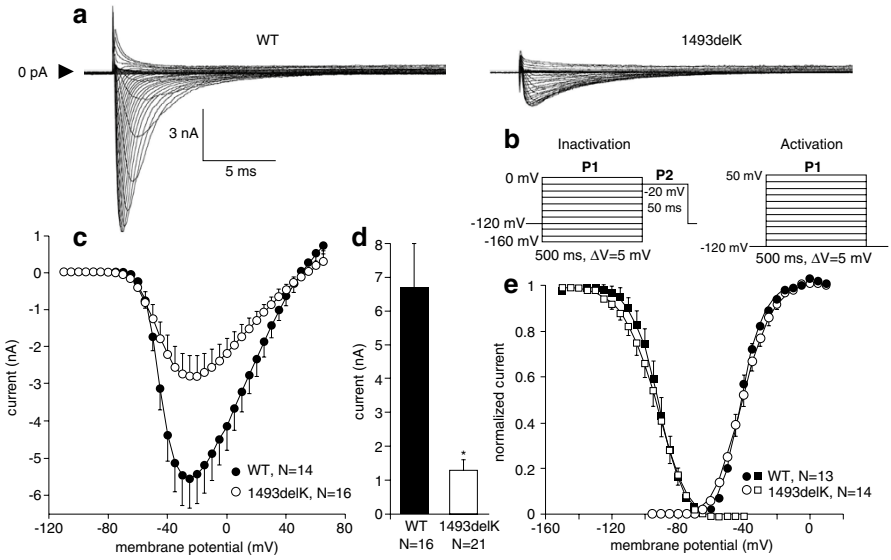


**Fig. 1.2** 1493delK mutant and wild-type (WT) human cardiac sodium channel current expressed in HEK293 cells [18]**.** (**a**) Whole-cell sodium current traces in response to increasing step depolarizations in WT (left) and 1493delK (right). (**b**) Voltage protocols for steady-state activation and inactivation. (**c**) Averaged current-voltage (I-V) relation for WT and 1493delK sodium channels. (**d**) Bar histogram showing averaged WT and 1493delK sodium peak currents at −20 mV. (**e**) Average voltage dependence of activation and steady-state inactivation for wild-type (WT) and 1493delK sodium channels. For the activation curve, normalized peak conductance was plotted as a function of the membrane potential. For the inactivation curve, peak sodium currents were normalized to maximum values in each cell and plotted as a function of the voltage of the conditioning step. (Reprinted from Zumhagen et al. [8]. Open Access)

steady-state activation and inactivation characteristics of this current are included in this figure. The currents were recorded in whole-cell patch clamp experiments in HEK293 cells expressing wild-type (WT) $Na_v1.5$ and 1493delK mutant $Na^+$ channels [18].

## Calcium Ion Channels

### Structure

The structure of voltage-gated $Ca^{2+}$ channels ($Ca_V$) is similar to that of $Na_v$ channels (Fig. 1.2) [22]. $Ca_V$ channels consist of a pore-forming *α-subunit* (α1) and at least two auxiliary subunits: *$\alpha_2\delta$- and* β-*subunits* [23]. Unlike cardiac or neuronal $Ca_V$ channels, a *γ-subunit* is also found in the skeletal muscle $Ca_V$ channel complex (Fig. 1.3) [24, 25]. The α1-subunit incorporates the voltage sensor and gating apparatus of $Ca_V$ channel and most of the known binding sites for channel regulators such as secondary messengers, drugs, and toxins [11]. The four glutamate residues (EEEE motif) in the α1-subunit of $Ca_V$ channels are responsible for $Ca^{2+}$ selectivity [26].

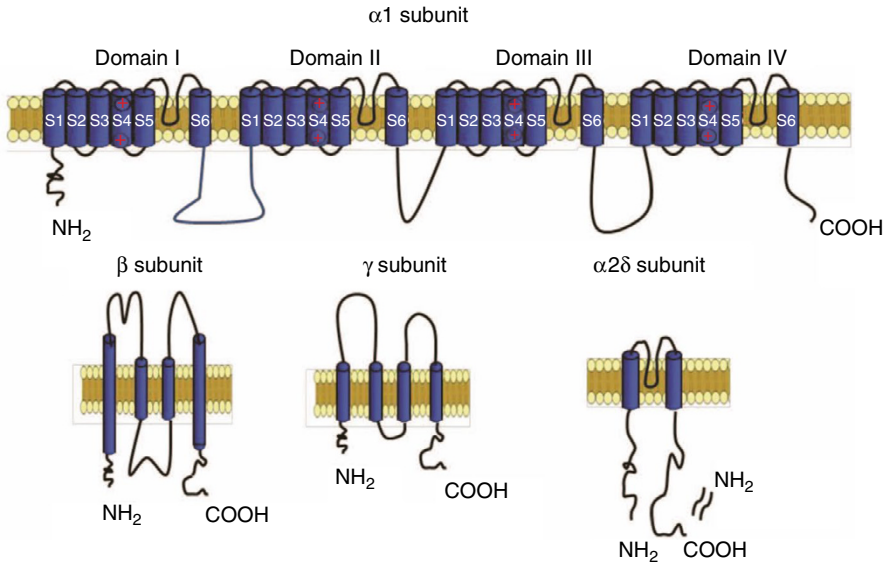


**Fig. 1.3** A schematic representation of voltage-gated $Ca^{2+}$ channels ($Ca_V$) [22]. The α1-subunit of $Ca_V$ channel demonstrates a similar structural basis to the $Na_V$ channels. The α2δ- and β-subunits enhance expression and modulate the voltage dependence and gating kinetics of the α1-subunit. (Reprinted from Huang et al. [22], with permission from Elsevier)

## Nomenclature and Family of $Ca_V$

Ten different $Ca_V$ channels have been identified to date based on their physiological and pharmacological properties. These channels are classified into three structurally and functionally related subfamilies primarily according to the difference in α1-subunits: $Ca_V1$, $Ca_V2$, and $Ca_V3$ (Table 1.3) [11]. The subtypes are named as below; take $Ca_V1.2$ as an example:

| $Ca_V1.2$ | | | |
|---|---|---|---|
| Ca | V | 1 | 2 |
| The principal permeating ion | The principal physiological regulator | The gene subfamily (1 to 3, at present) | The order of discovery of the α1-subunit within that subfamily (1 through n) |

The $Ca_V1$ subfamily mediates L-type $Ca^{2+}$ currents (L – long-lasting and large conductance). The $Ca_V2$ subfamily mediates P/Q-type $Ca^{2+}$ currents (P/Q – Purkinje cells), N-type $Ca^{2+}$ currents (N – neuron pre-synapse), and R-type $Ca^{2+}$ currents (R – resistant to peptide toxins). The $Ca_V3$ subfamily mediates T-type $Ca^{2+}$ currents (T – transient-opening and small conductance) [26].

For detailed information on $Ca_V$ channels such as gene and protein information, voltage dependence, channel activator and inhibitor, channel blockers, species and tissue distribution, and clinically relevant mutations and pathophysiology, please refer to the International Union of Basic and Clinical Pharmacology (IUPHAR) voltage-gated calcium channels database [27].

**Table 1.3** Summary of human voltage-gated calcium channels [11, 22, 26]

| Current type | α1-Subunits | Gene | Tissue distribution | Specific blocker | Principal functions |
|---|---|---|---|---|---|
| L | $Ca_V1.1$ ($\alpha_{1S}$) | CACNA1S | Skeletal muscle, transverse tubules | DHPs | Excitation-contraction coupling in skeletal muscle, regulation of transcription |
| L | $Ca_V1.2$ ($\alpha_{1C}$) | CACNA1C | Cardiomyocytes, smooth muscle myocytes, endocrine cells, neuronal cell bodies, proximal dendrites | DHPs | Excitation-contraction coupling, hormone release, regulation of transcription, synaptic integration |
| L | $Ca_V1.3$ ($\alpha_{1D}$) | CACNA1D | Endocrine cells, neuronal cell bodies and dendrites, cardiac atrial myocytes and pacemaker cells, cochlear hair cells | DHPs | Endocrine secretion, cardiac pacemaking, neuronal $Ca^{2+}$ transients in cell bodies and dendrites, auditory transduction |
| L | $Ca_V1.4$ ($\alpha_{1F}$) | CACNA1F | Retinal rod and bipolar cells, spinal cord, adrenal gland, mast cells | DHPs | Visual transduction |
| P/Q | $Ca_V2.1$ ($\alpha_{1A}$) | CACNA1A | Nerve terminals and dendrites, neuroendocrine cells | ω-CTx-GVIA | Neurotransmitter release Dendritic $Ca^{2+}$ transients |
| N | $Ca_V2.2$ ($\alpha_{1B}$) | CACNA1B | Nerve terminals and dendrites, neuroendocrine cells | ω-Agatoxin | |
| R | $Ca_V2.3$ ($\alpha_{1E}$) | CACNA1E | Neuronal cell bodies and dendrites | SNX-482 | |
| T | $Ca_V3.1$ ($\alpha_{1G}$) | CACNA1G | Neuronal cell bodies and dendrites, cardiac and smooth muscle myocytes | – | Pacemaking and repetitive firing |
| T | $Ca_V3.2$ ($\alpha_{1H}$) | CACNA1H | Neuronal cell bodies and dendrites, cardiac and smooth muscle myocytes | – | |
| T | $Ca_V3.3$ ($\alpha_{1I}$) | CACNA1I | Neuronal cell bodies and dendrites | – | |

DHP (dihydropyridine), ω-CTx-GVIA (conotoxin GVIA from the cone snail *Conus geographus*), SNX-482 (a synthetic version of a peptide toxin from the tarantula *Hysterocrates gigas*)

### L-Type ($Ca_V1.x$) and T-Type ($Ca_V3.x$) Channels

Both the L-type and T-type $Ca^{2+}$ channels play key roles in the heart. The *L-type $Ca^{2+}$ channels* are typically activated during the depolarization of the cell and remain in the active state for longer periods relative to $Na_v$ channels. They are the main channels conducting $Ca^{2+}$ions into cardiac cells (the corresponding current is $I_{Ca,L}$). After the initiation of the cardiac action potential, $I_{Ca,L}$ is rapidly activated

and takes a few milliseconds to reach peak value. During activation, the inward $Ca^{2+}$ currents continuously contribute to the sustained plateau phase of cardiac action potential. The increase of intracellular calcium concentration ($[Ca^{2+}]_i$) then gives rise to $Ca^{2+}$ release from the sarcoplasmic reticulum via type 2 ryanodine receptors (RyR2) (*$Ca^{2+}$-induced $Ca^{2+}$ release*). As a result, a great amount of $Ca^{2+}$ions are dumped into the cytoplasm which then bind to the myofilaments and initiate cardiac contraction [2].

The binding of $Ca^{2+}$ to the carboxyl terminus of the L-type $Ca^{2+}$ channels contributes to channel inactivation. When the cell begins to repolarize, the fraction of the inactivated L-type $Ca^{2+}$ channels increases. The re-uptake of intracellular $Ca^{2+}$ by the sarcoplasmic reticulum and the extrusion of $Ca^{2+}$ via Na-Ca exchanger together result in the recovery of L-type $Ca^{2+}$ channels from inactivated phase to resting phase getting them ready for the next stimulus [2].

L-type $Ca^{2+}$ channel mutations have been related to cardiac diseases such as Timothy syndrome (TS). TS is a multi-organ system disease which can manifest as long QT interval, cognitive abnormalities, syndactyly, and sudden cardiac death (SCD) [28]. Such a mutation is caused by a glycine to arginine substitution at position 406 (G406R) of the human $Ca_V1.2$ channel. The phosphorylation of this mutant site can result in the slow gating of $Ca_V1.2$ channel and in increased $Ca^{2+}$ entry [29].

*T-type $Ca^{2+}$ currents* are activated by weak depolarization, in the same membrane potential range as $Na^+$ currents in most cells, and their activation is transient. These channels are involved in shaping the action potential and modulating excitability and repetitive firing of the cells (automaticity) in which they are expressed. For example, in the SA node and AV node, $Ca_V3.1$ and $Ca_V3.2$ channels conduct an important component of the pacemaking current that generates the heartbeat [30, 31].

Figure 1.4 illustrates the $Ca^{2+}$ current-voltage (I-V) relationships and the corresponding steady-state inactivation curve recorded in whole-cell patch clamp experiments using mice cardiac pacemaker cells.

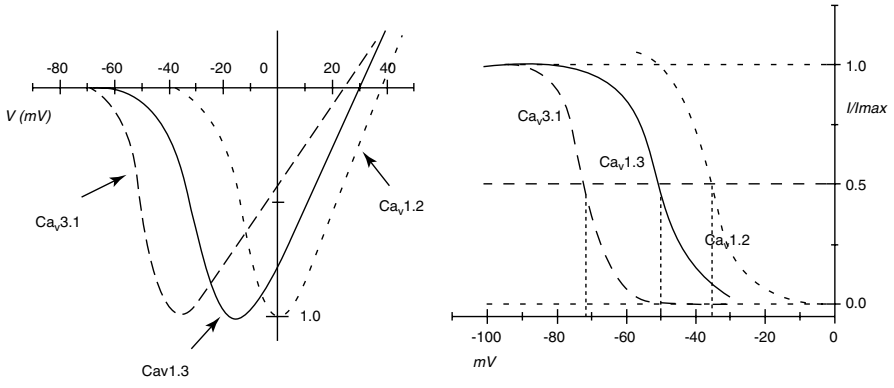


**Fig. 1.4** Properties of voltage-gated $Ca^{2+}$ channels in mice cardiac pacemaker cells [32]**.** I–V curve (left) and steady-state inactivation (right) of native SA node. $Ca_v3.1$ (dashed curve), $Ca_v1.3$ (solid curve), and $Ca_v1.2$ (dotted curve). (Reprinted from Mangoni et al. [32], with permission from Elsevier)

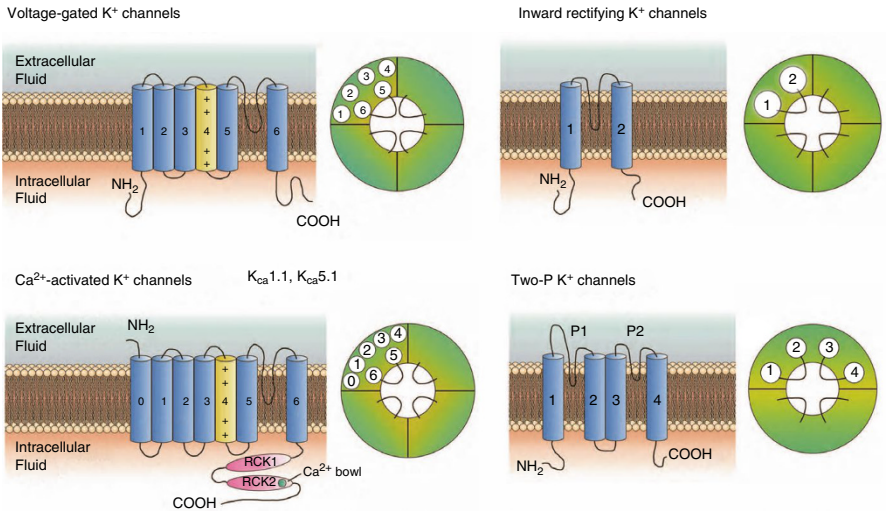


**Fig. 1.5** Schematic structure of the four main K+ channel. Schematic representation of the four types of potassium ion channels

## Potassium Ion Channels

Potassium channels possess the most functional diversity among all cardiac ion channel types. Based on the topology of pore-forming structures (i.e., α-subunits), $K^+$ channels can be classified into four main groups – *voltage-gated $K^+$ channels*, *$Ca^{2+}$-activated $K^+$ channels*, *inwardly rectifying $K^+$ channels*, *and two pore $K^+$ channels* (Fig.1.5) [33–35].

### Cardiac Potassium Channels

Cardiac $K^+$ channels are important for the repolarization of the cardiomyocyte. The differences in the type and/or expression patterns of various $K^+$ channels largely account for the region-specific morphology of cardiac action potential (AP) in the atria, in the ventricles, and across the myocardial wall [36]. $K^+$ channels are also the pharmacological targets for class III anti-arrhythmic drugs that are used to prevent or suppress cardiac arrhythmias. There are three groups of $K^+$ channels expressed in the human heart: *voltage-gated channels*, *inwardly rectifying channels*, and *two pore domain channels* (Table 1.4) [37–40].

#### Voltage-Gated Potassium Channel Structure

There are 40 human voltage-gated $K^+(K_v)$ channel genes belonging to 12 subfamilies. These channels possess a large pore-forming α-subunit composed of four domains: either identical (homomultimers) or different domains from the same subfamily (heteromultimers) [41]. Each domain of the α-subunit consists of six transmembrane peptide segments (S1–S6). The pore of the $K_v$ channels contains the channel gates and a $K^+$ selective filter. The pore loop between S5 and S6 with a

**Table 1.4** Cardiac potassium channels [37–40]

| Group | Current | | α-Subunit | Gene (human) | AP phase |
|---|---|---|---|---|---|
| Voltage-gated $K^+$ channels | $I_{tof}$ | Fast transient outward $K^+$ current | $K_V4.3$ | KCND3 | Phase 1 |
| | $I_{tos}$ | Slow transient outward $K^+$ current | $K_V1.4$ | KCNA4 | Phase 1 |
| | $I_{Kur}$ | Ultra-rapid component of the delayed rectifier $K^+$ current | $K_V1.5$ | KCNA5 | Phase 1 |
| | $I_{Kr}$ | Rapid component of the delayed rectifier $K^+$ current | $K_V11.1$ | KCNH2 | Phase 3 |
| | $I_{Ks}$ | Slow component of the delayed rectifier $K^+$ current | $K_V7.1$ | KCNQ1 | Phase 3 |
| Inwardly rectifying $K^+$ channels | $I_{K1}$ | Inwardly rectifying $K^+$ channels (strong rectifying) | $K_{ir}2.1$ / $K_{ir}2.2$ | KCNJ2 / KCNJ12 | Phase 3 & 4 |
| | $I_{KACh}$ | Acetylcholine-activated $K^+$ channels (strong rectifying) | $K_{ir}3.1$ / $K_{ir}3.4$ | KCNJ3 / KCNJ4 | Phase 4 |
| | $I_{KATP}$ | Adenosine triphosphate-sensitive $K^+$ currents (weak rectifying) | $K_{ir}6.1$ / $K_{ir}6.2$ | KCNJ8 / KCNJ11 | Phase 1 & 2 |
| Two-pore domain $K^+$ channel | $I_{KP}$ (a.k.a$I_{leak}$) | Background (or leak) $K^+$ currents | $K_{2P}3.1$ | KCNK3 | All phases |

consensus amino acid sequence, -TxxTxGYGD- (-thr-X-X-thr-X-gly-tyr-gly-glu-), is responsible for the $K^+$ selectivity and forms the upper (extracellular) gate comprising the extracellular pore of $K_V$ channels [35], while the lower (intracellular) gate is formed by crossing C-termini of the S6 helices at the intracellular entrance of the pore that blocks ion flux when the channel is closed [42]. The S4 segment contains regular repeats of positively charged amino acids at every third position which makes S4 segment the voltage sensor that moves in response to membrane potential change [43]. There are auxiliary subunits (β-subunits) that form complexes with the α-subunits and modify the channel functions. For example, $K_V$ β-subunits can alter the voltage dependence of $K_V1.5$ channel opening [44]. $K_v$ channels also include the complementary proteins: $K_V$ channel-associated protein (KChAP) and the $K_V$ channel-interacting protein (KChIP) [39].

$K_V$ channels can be presented in three functional states: resting (closed), activated (open), and inactivated (closed). Immediately after depolarization, $K_V$ channels switch from resting state to open state as a result of conformational rearrangement of channel pore. After activation, many $K_V$ channels switch to inactivated state leading to a decline in repolarizing current. When the membrane is repolarized back to RMP, $K_V$ channels recover from the inactivated state and are capable of being activated by the next depolarization stimulus [42].

Three *mechanisms of inactivation* have been described in $K_v$ channels so far: the first two involve the conformational constriction of the ion conductance pore, and the third involves occlusion of the pore by an auto-inhibitory part of the channel protein (Fig.1.6) [45]. In the first mechanism, four intracellular S6 segments (*intracellular gate*) swing together to produce a secure closure of the channel pore from

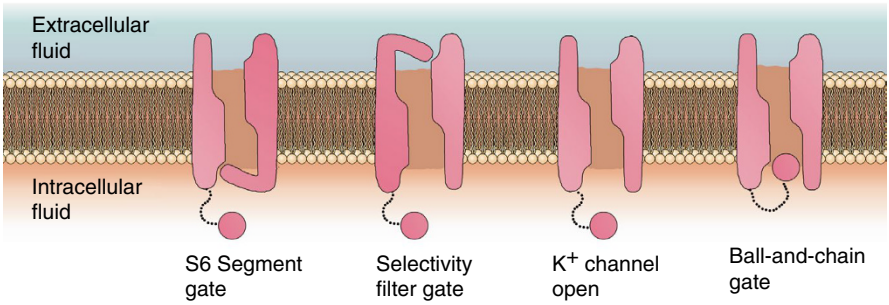


**Fig. 1.6** Inactivation mechanisms of voltage-gated $K^+$ channels**.** From left to right: channel closed as the S6 segment swings toward the pore from intracellular side, channel closed as the selectivity filter blocks the pore, channel open during activation, and the occlusion of the pore via ball-and-chain mechanism

cytoplasmic side. This mechanism is important for its interaction with channel blockers. For example, some small organic blockers can enter the channel only after the activation of channel and can be trapped inside the pore when S6 closes [46, 47]. In the second mechanism, the extracellular $K^+$ selective filter acts as a gate and closes the pore (i.e., *C-type inactivation*). Closure of this gate can be prevented by the binding of extracellular tetraethylammonium ion (TEA) to the pore [48]. The third mechanism, *fast N-type inactivation* (as it is faster than C-type inactivation), involves the occlusion of cytoplasmic opening of the channel pore by the intracellular (N-terminal) auto-inhibitory peptide. This occurs only while the S6 gate is open and is also called as the ball-and-chain mechanism.

### Voltage-Gated Potassium Channel Currents

The *transient outward current* ($I_{to}$) is rapidly activated and inactivated in response to depolarization. $I_{to}$ is composed of a voltage-dependent $K^+$ current ($I_{to1}$) and a $Ca^{2+}$-activated chloride ($Cl^-$) current ($I_{to2}$) [49]. Based on the voltage-dependent kinetics of recovery from inactivation, $I_{to1}$ is further classified into fast ($I_{tof}$, with recovery time constant of approximately 30–100 ms) and slow ($I_{tos}$, with recovery time constant of approximately 100–1000 ms) $K^+$ current [50]. $I_{tof}$ can be distinguished from $I_{tos}$ by differential sensitivity to the $K^+$ channel toxins such as *Heteropoda* toxins (HPTXs) that blocks $I_{tof}$ but not $I_{tos}$ at nanomolar concentrations [51]. $I_{tof}$ is the principal $I_{to}$ current in human atria, while both $I_{tof}$ and $I_{tos}$ have been described in the ventricles. These two currents account for the early rapid repolarization of cardiomyocytes and determine the amplitude of the early plateau phase of the AP [33]. Regions with shorter action potential durations, such as the epicardium, right ventricle, and septum, have higher $I_{to}$ expression. In large mammals including humans, a reduction of $I_{to1}$ elevates the plateau phase to more positive potentials.

In humans and other large mammals, the cardiac *delayed rectifier $K^+$ currents* ($I_{Kr}$) are responsible for repolarization. $I_{Kr}$ involves three different components: the

*ultra-rapid ($I_{Kur}$)*, the *rapid ($I_{Kr}$)*, and the *slow ($I_{Ks}$)* activating components. These channels deactivate sufficiently slowly such that they contribute to outward $K^+$ currents throughout repolarization. Because of their partly overlapping functions, they contribute to the *repolarization reserve* [40].

$I_{Kur}$ is expressed almost exclusively in atria and is responsible for the much shorter duration of the atrial action potential compared to that of the ventricles [52]. $I_{Kr}$ is highly expressed in the left atrium and ventricular endocardium. $I_{Ks}$ is expressed in all cardiac cell types but with a reduced expression level in midmyocardial myocytes which have the longest action potential duration across the myocardial wall [53]. $I_{Kr}$ and $I_{Ks}$ can be separated based on their different sensitivity to drugs. For example, $I_{Kr}$ can be blocked by E-4031, and $I_{Ks}$ can be blocked by chromanol 293B or L-735,821 [54, 55].

$I_{Kr}$ activates rapidly upon depolarization; however, its inactivation rate is approximately tenfold faster at positive potentials due to voltage-dependent C-type inactivation. This limits the amount of time $I_{Kr}$ channels are in open state. $I_{Kr}$ displays an inverted bell-shaped I-V relationship because of rapid inactivation, with current peaking at potentials ranging between 0 and + 10 mV [56]. Upon repolarization, $I_{Kr}$ channels are released from inactivation to open state.

$I_{Ks}$ activates relatively slower than $I_{Kr}$. The time constant of activation of $I_{Ks}$ is in the order of seconds, while that of $I_{Kr}$ is tens or hundreds of milliseconds [57]. After the slow activation at potentials positive to −20 mV, $I_{Ks}$ inactivates extremely slowly such that its I-V relationship is almost linear and, therefore, $I_{Ks}$ accumulates gradually during phase 2 repolarization and conducts strong outward $K^+$ currents in phase 3 repolarization [58]. $I_{Ks}$ also contributes to the action potential duration shortening during physiological increases in heart rate. The increase in heart rate allows less time for $I_{Ks}$ to inactivate, leading to an accumulation of open $I_{Ks}$ channels and a faster repolarization rate [59]. The blocking of $I_{Ks}$ can result in the prolongation of APD at higher heart rate [60].

### Inwardly Rectifying Potassium Channel Structure

There are 15 types of inwardly rectifying $K^+$ channels ($K_{ir}$) in humans, belonging to 7 subfamilies. The direction of current is defined by the direction of flux of positive charge. For example, the flux of $Na^+$ into a cell is called an inward current, and the flux of $K^+$ out of a cell is called an outward current, while the flux of $Cl^-$ into a cell is also called an outward current. *Outward rectification* occurs when the outward current flows more easily than the inward current (net positive charge out of a cell). *Inward rectification* occurs when the inward current flows more easily than the outward current (net positive charge into a cell).

First identified in skeletal muscle, $K_{ir}$ currents were originally described as "anomalous" rectifier $K^+$ currents as they showed greater inward current than outward current. To date, $K_{ir}$ channels have been found in cardiomyocytes, neurons, blood cells, osteoclasts, endothelial cells, glial cells, epithelial cells, and oocytes [61]. Strong $K_{ir}$ currents play a significant role in stabilizing the RMP and the resultant cell electrical excitability, while weak $K_{ir}$ channels are critical for both setting RMP and shortening action potential.

The $K_{ir}$ family has the simplest structure among $K^+$ channels. Each of the four (homo- or hetero-) domains of the α-subunit consists of only two transmembrane segments (TM1 and TM2) that are connected by an extracellular pore loop structure and cytoplasmic amino (NH2)- and carboxy (COOH)- terminal domains [62, 63]. The pore loop works as the ion selective filter similar to other $K^+$ channels and has the signature sequence T-X-G-Y(F)-G [64]. Because of the lack of an S4 segment that serves as voltage sensor, $K_{ir}$ channels are insensitive to changes in membrane potential and have distinct voltage-independent mechanisms for opening and closing such as in ATP-sensitive $K^+$ channels ($K_{ATP}$) that open in response to a decrease in intracellular ATP and G protein-gated $K^+$ channels ($K_G$) that activate via pertussis toxin (PTX)-sensitive G proteins. When such channel-regulating mechanisms are absent, $K_{ir}$ channels would be active at all membrane potentials [65–67]. The physiological function of $K_{ir}$ channels can be regulated by intracellular $Mg^{2+}$ and polyamines, extracellular $K^+$ concentrations, membrane-anchored phosphatidylinositol 4,5-bisphosphate, and intracellular and/or extracellular pH. The localization of $K_{ir}$ channels in specific regions of a cell is also important for channel functions [61, 68, 69].

In physiological conditions, $K_{ir}$ channels conduct large inward $K^+$ currents at potentials negative to the equilibrium potential of $K^+$ ($E_K$, approximately −96 mV) and smaller currents at potentials positive to $E_K$ [70, 71]. This property of conducting greater inward $K^+$ currents than outward $K^+$ currents when activated makes $K_{ir}$ channels critical for maintaining the RMP and for repolarization [72]. Cells with higher expression of $K_{ir}$ channels are expected to have an RMP close to $E_K$. Increasing the concentration of extracellular potassium shifts the peak of the outward current to more depolarized potentials.

### Inwardly Rectifying Potassium Currents

The inwardly rectifying $K^+$ channels ($K_{ir}$) derive their name ("inwardly rectifying") from the current-voltage relationship because the inward current is typically much larger than the outward current. Another property of $K_{ir}$ channels is that the increase of extracellular $K^+$ concentration shifts the peak of the outward $K^+$ current to more positive potentials nearly in parallel with the equilibrium potential of $K^+$ (i.e., $E_K$) leading to a "crossover" phenomenon (Fig. 1.2b). As a result, at potentials positive to the crossover point, outward $K^+$ conductance increases rather than decreases, despite an increase in driving force [73].

At physiological conditions $K_{ir}$ channels conduct outward $K^+$ currents contributing to the late part of repolarization. When membrane potential becomes more negative than $E_K$, $K_{ir}$ channels conduct inward $K^+$ currents to clamp the RMP. Therefore, $K_{ir}$ channels are critical for stabilizing the RMP. This is emphasized by the fact that the RMP is approximately −90 mV for ventricular cardiomyocytes with high $K_{ir}$ channel expression, while "RMP" is approximately −50 mV for nodes lacking $K_{ir}$ channels [74]. The $K_{ir}$ channels include seven subtypes of which the *Kir2.x*, *Kir3.x*, and *Kir6.x* are expressed in the heart [62].

The *$K_{ir}$2.x channels* are classified as strong inwardly rectifying channels. $K_{ir}2.1$ is the predominant isoform of $I_{K1}$ channels in ventricular myocytes while $K_{ir}2.3$ is